HHS Public Access

Author manuscript

*J Immunol*. Author manuscript; available in PMC 2019 August 01.

Published in final edited form as:

*J Immunol*. 2018 August 01; 201(3): 1030–1043. doi:10.4049/jimmunol.1800188.

# Ligation of the CD44 Glycoform HCELL on Culture-Expanded Human Monocyte-derived Dendritic Cells Programs Transendothelial Migration

**Paula A. Videira**[1,2,3], **Mariana Silva**[2,4,5], **Kyle C. Martin**[4,5], and **Robert Sackstein**[4,5,*]

[1]UCIBIO, Departamento Ciências da Vida, Faculdade de Ciências e Tecnologia, Universidade NOVA de Lisboa, Caparica, Portugal

[2]Centro de Estudos de Doenças Crónicas, CEDOC, NOVA Medical School / Faculdade de Ciências Médicas, Universidade NOVA de Lisboa, Lisboa, Portugal

[3]CDG & Allies – Professionals and Patient Associations International Network (CDG & Allies – PPAIN), Caparica, Portugal

[4]Departments of Dermatology and of Medicine, Brigham and Women's Hospital, Boston, MA 02115, USA

[5]Program of Excellence in Glycosciences, Harvard Medical School, Boston, MA 02115, USA

## Abstract

The success of dendritic cell (DC)-based immunotherapeutics critically hinges on the capacity of the vascularly administered cells to enter tissues. Transendothelial migration (TEM) is dictated by an ordered cascade of receptor/ligand interactions. Here, we examined the key molecular effectors of TEM of human mo-DCs generated by clinically-relevant methods: CD14-selection (CD14-S) and plastic adherence-selection (PA-S). Without chemokine input, CD14-S cells undergo greater TEM than PA-S cells over TNFα-stimulated HUVECs. TEM of CD14-S mo-DCs is E-selectin/VLA-4-dependent, and engagement of E-selectin ligands activates VLA-4 on CD14-S mo-DCs but not on PA-S mo-DCs. E-selectin binding glycoforms of PSGL-1 (i.e., CLA) and CD44 (i.e., HCELL) are both expressed on CD14-S mo-DCs but only CLA is expressed on PA-S mo-DCs. To elucidate the effect of CD44 or PSGL-1 engagement, mo-DCs were pre-treated with their ligands. Ligation of CD44 on CD14-S mo-DCs triggers VLA-4 activation and TEM, whereas PSGL-1 ligation does not. HCELL expression on CD14-S mo-DC can be enforced by cell surface exofucosylation, yielding increased TEM *in vitro* and enhanced extravasation into bone marrow *in vivo*. These findings highlight structural and functional pleiotropism of CD44 in priming TEM of

*Corresponding Author: Robert Sackstein, MD, PhD, Harvard Institutes of Medicine, 77 Ave Louis Pasteur, Room 671, Boston, MA 02115, Phone 617-525-5604; Fax 617-525-5571, rsackstein@rics.bwh.harvard.edu.

**Author contributions:** The study was conceived by both R.S. and P.V. R.S. designed and supervised all research, funded the research and wrote the manuscript. P.V. designed and performed research, collected and analyzed data, and wrote the manuscript. M.S. designed and performed research, collected and analyzed data, and wrote the manuscript. K.C.M. performed research.

**Competing interests:** According to NIH policies and procedures, the Brigham & Women's Hospital has assigned intellectual property rights regarding HCELL, and the glycan engineering technology ("glycosyltransferase-programmed stereosubstitution" (GPS)) to enforce HCELL expression, to the inventor (R.S.) who may benefit financially if the technology is licensed. R.S.'s ownership interests were reviewed and are managed by the Brigham and Women's Hospital and Partners HealthCare in accordance with their conflict of interest policy.

mo-DCs and suggest that strategies to enforce HCELL expression may boost TEM of systemically-administered CD14-S mo-DCs.

**Keywords**

Dendritic cell; Cell Migration; E-selectin Ligand; Hematopoietic Cell E-selectin/L-selectin Ligand (HCELL); Immunotherapy; Fucosyltransferase; Glycosyltransferase-Programmed Stereosubstitution (GPS); Sialyl Lewis X; Tumor Necrosis Factor-α

## Introduction

The adaptive immune system is orchestrated by T lymphocytes whose functions are governed by “professional’ antigen presenting cells such as dendritic cells (DCs). DCs are bone marrow-derived leukocytes that are specialized to capture, process, and present antigens to T cells, thereby coordinating immune responses by activating naïve and memory T cells (1). Though DCs are a very minor population of circulating leukocytes, techniques have been developed to culture-expand these cells from peripheral blood monocyte precursors (“mo-DCs”), and, therefore, sufficient quantities of these cells can be generated *in vitro* to enable DC-based adoptive immunotherapeutics (2).

To date, mo-DCs used in clinical trials are derived from precursor monocytes enriched from human blood using two well-established methods: plastic adherence (PA-S) [e.g., clinical trials NCT00085397, NCT00045968, and NCT01067287] and CD14-selection (CD14-S) [e.g., clinical trials NCT00834002, NCT00814892, and NCT01525017]. Whether “pulsed” (antigen-loaded) or not, it is critical that culture-expanded DCs gain access to lymph nodes, wherein DCs engage both naive and memory T cells in anatomically specialized microenvironments that enable the proper scope of antigen stimulation. However, mo-DCs generated *in vitro* behave like "conventional" DCs in that these cells cannot enter lymph nodes from blood (i.e., they do not extravasate across lymph node high endothelial venules (HEVs) (3)). Apart from this HEV-based migration route, DCs can enter nodes via a circuit that requires initial peripheral tissue residency and emigration therefrom via afferent lymphatics. However, previous studies have also indicated that *in vitro*-generated systemically-administered DCs have deficient tissue migration and, consequently, poor lymph node accumulation, thus markedly lessening their efficacy in adoptive DC-based immunotherapeutics (4–6). In attempt to overcome this shortfall, clinical trials have been designed whereby DCs are directly injected into tissues, from which they can then migrate through afferent lymphatics and thereby enter the draining lymph node (6) [e.g., clinical trials NCT01863108, NCT02018458]. Though seemingly straightforward, this approach is hampered in that only limited numbers of cells can be introduced locally and the attendant procedure-related disruption of tissue integrity *in situ* could affect the architecture of the draining lymphatics. Thus, for use of DCs in clinical immunotherapeutics, a better understanding of the molecular effectors of DC extravasation is needed, and strategies must be developed to maximize the efficiency of this process.

Extravasation of blood-borne cells involves a multistep cascade of events initiated by hemodynamic shear-resistant adhesion of cells to target endothelium. This important

function is mediated most efficiently by engagement of selectins with sialofucosylated glycans that are displayed on cell surface protein or lipid scaffolds, prototypically consisting of the tetrasaccharide sialyl Lewis X (sLe$^x$; NeuAc-α(2,3)-Gal-β(1,4)-[Fuc-α(1,3)]GlcNAc-R) (7). The vascular selectins are comprised of E- and P-selectin. In humans, E-selectin is expressed constitutively within bone marrow microvessels and is inducible on all endothelial cells by inflammatory cytokines, thus mediating recruitment of leukocytes into bone and all inflammatory sites (8, 9). Sialofucosylated ligands for vascular selectins serve as tissue "homing receptors" on circulating cells, and mediate tethering and rolling of the cells on the endothelium (Step 1). The cells then undergo "Step 2" activation of integrin adhesiveness, typically via chemokine receptor signaling, leading to firm adhesion on the endothelium (Step 3), and then transendothelial migration (TEM) (Step 4) (7). Importantly, the principal inflammatory cytokines, tumor necrosis factor-α (TNFα) and interleukin (IL)-1β, upregulate both E- and P-selectin expression in murine endothelial cells, but the promoter elements responsive to TNFα and IL-1β in the human P-selectin gene are absent (10). Thus, in humans, E-selectin receptor/ligand interactions play a predominant role in recruitment of blood-borne cells to inflammatory sites, prompting development of strategies to enforce E-selectin ligand expression on relevant human cells to optimize their utility in adoptive immunotherapeutics.

The molecular effectors mediating DC adherence to endothelium and consequent TEM have not been fully elucidated. To date, P-selectin glycoprotein ligand-1 (PSGL-1) is the only sLe$^x$ scaffold reported to be expressed on human DCs, and PSGL-1 is the principal P-selectin counterreceptor in human mo-DCs (11–13). Though a heavily sialofucosylated glycoform of PSGL-1 that binds E-selectin (known as "Cutaneous Lymphocyte Antigen" (CLA)) has been described on DCs (11), our knowledge of the breadth and function of human mo-DC glycoconjugate counterreceptors for E-selectin is incomplete. In humans, hematopoietic stem cells express a CD44 glycoform known as Hematopoietic Cell E-selectin/ L-selectin Ligand (HCELL) (14, 15), which serves as a potent E-selectin ligand. CD44 expression is characteristic of human DCs and is known to be critical for DC lodgment within T cell zones of lymph nodes and formation of immunological synapses (16, 17), but its role in mediating recruitment of blood-borne DC into tissues has not been evaluated.

In this study, we examined TEM of human blood mo-DCs on primary cultures of human umbilical vein endothelial cells (HUVECs) treated with TNFα to mimic inflammation-related endothelial expression of E-selectin and of vascular cell adhesion molecule-1 (VCAM-1), another TNFα-induced molecule that serves as a ligand for integrin very late antigen-4 (VLA-4). We observed that CD14-S or PA-S mo-DCs can each execute TEM in absence of applied chemokine gradients, but CD14-S mo-DCs transmigrate with greater efficiency than do PA-S cells. Our results indicate that TEM is dependent on engagement of mo-DC E-selectin ligands, and that whereas both CD14-S mo-DCs and PA-S mo-DCs express CLA, CD14-S mo-DCs also express HCELL. We observed that engagement of HCELL on CD14-S mo-DCs directly activates VLA-4 thereby programming TEM on TNFα stimulated HUVECs, and, also, that enforced HCELL expression by α-(1,3)-exofucosylation of CD44 on CD14-S mo-DC significantly enhances TEM. Collectively, these findings unveil a molecular axis that drives human DC TEM, expose a previously unrecognized structural

and functional versatility of CD44 on human DCs, and suggest that glycosylation of CD44 to engender HCELL expression may be exploited to enable tissue delivery of systemically-administered culture-expanded human DCs.

## Materials and Methods

### Cell isolation and culture

Human peripheral blood mononuclear cells (PBMCs) were isolated from blood of healthy donors obtained by venipuncture, under protocols approved by the Institutional Review Board of Brigham & Women's Hospital, with Informed Consent provided as per the Declaration of Helsinki. Blood monocytes were enriched using anti-CD14 mAb-coated magnetic beads (Miltenyi Biotech, Bergisch Gladbach, Germany) (CD14-S) or by plastic adherence (PA-S), and differentiated by culturing them in 1000 U/ml IL-4 and 1000 U/ml GM-CSF for 5 days as previously described (18, 19). After 5 days of differentiation, the mo-DCs were then "matured" by culturing with TNFα (25 ng/mL, R&D Systems) for 2 or 3 days (as specified), or left untreated ("immature" DCs), in each case treated with 1000 U/ml IL-4 and 1000 U/ml GM-CSF. For activation, mo-DCs were treated with 200 ng/ml of phorbol 12-myristate 13-acetate (PMA, Sigma, Saint Louis, MO, USA) in RPMI media for 30 min at 37°C. HUVECs were obtained from the BWH Pathology Core facility and cultured as described (13, 20).

### Antibody reagents and flow cytometry

Monocyte purity was evaluated by flow cytometry for expression of CD14, and differentiation and maturation of mo-DCs were evaluated by staining for expression of MHC-II, and CD86 (mAbs from BD Biosciences, San Jose, CA, USA). Anti-CD44 mAb 2C5 and recombinant mouse E-selectin-human Fc Ig chimera (E-Ig) were from R&D Systems, Minneapolis, MN, USA. HECA-452, anti-CD29 and anti-CD49d mAbs were from BD Biosciences. Activation-dependent epitopes of VLA-4 and LFA-1 were evaluated using mAb HUTS-21 (specific for β1 chain (CD29) (BD Biosciences)) and mAb 24 (specific for integrin β2 (CD18) chain of CD11/CD18 heterodimers (Hycult Biotech, Plymouth Meeting, PA, USA)), respectively.

### Blot Rolling Assay

Western blots of PVDF membrane preparations stained with anti-CD44 were rendered transparent with Hanks balanced salt solution (HBSS) containing 2 mM $Ca^{2+}$ and 10% glycerol and were placed in the parallel plate flow chamber. Chinese hamster ovary (CHO) cells transfected with full-length human E-selectin cDNA (CHO-E) were suspended ($10^6$ cells/mL) in HBSS containing 2 mM $Ca^{2+}$ and perfused over blots at 1.4 dyn/$cm^2$ and incremented up to 4.2 dyn/$cm^2$. The number of cells rolling within and outside relevant immunostained bands of the blot were recorded and quantified within each field of view by video microscopy. Controls for non-specific binding consisted of CHO-E cells in media containing 5 mM EDTA (chelating $Ca^{2+}$ to prevent E-selectin adhesion), and incubation of CHO-E cells in presence of function-blocking anti-E-selectin mAb (clone 68-5H11; from B-D Biosciences). Mock transfectants (CHO-mock) were used as control to analyze background levels of CHO adhesive interactions on blots.

### Isolation of RNA and Real-Time PCR

Total RNA was extracted and reverse transcribed as described (18). Real-Time PCR (RT-PCR) was performed using SYBR Green PCR Master Mix (Applied Biosystems, Foster City, CA, USA). Primers were selected from PrimerBank (21) and for each gene the forward Primer (5'–3') and Reverse Primer (5'–3') were as following. *FTIV*: GATCTGCGCGTGTTGGACTA, GAGGGCGACTCGAAGTTCAT; *FTVI*: GCGTGTGTCTCAAGACGATCC, GGAAGCGGGACCCATTAGG; *FTVII*: CACCTGAGTGCCAACCGAA, CACCCAGTTGAAGATGCCTCG; *C2GnT1*: AACCCCTTAGTAAAGAAGAGGCG, AGCAGCCTGTCAAGCATTTCA; *ST3GalI*: AAGAGGACCCTGAAAGTGCTC, CTCCAGGACCATCTGCTTGG; *ST3GalIII*: GCCTGCTGAATTAGCCACCAA; GCCCACTTGCGAAAGGAGT; *ST3GalIV*: CTTCCTGCGGCTTGAGGATTA, CTCACTCCCCTTGGTCCCATA; *ST3GalVI*: ACTGCATTGCATATTATGGGGAA, TGGCTTTGATAAACAAGGCTGG; *ST6GalNAcII*: ACTTCCGTGGCCTGTTCAATC, GGCGATGACTTGGTGAGAGAG; *Neu1*: GGAGGCTGTAGGGTTTGGG, CACCAGACCGAAGTCGTTCT; *Neu3*: AAGTGACAACATGCTCCTTCAA, TCTCCTCGTAGAACGCTTCTC, in each case, gene expression was normalized to *GAPDH* (endogenous reference) expression. The normalized mRNA expression was computed as a permillage fraction (‰), which means the proportion of target mRNA per thousand of the reference *GAPDH* mRNA expression, calculated by using the $2^{-\Delta CT}\times 1000$ formula (22, 23). Amplification specificity was confirmed by melting curve analysis.

### Transendothelial migration (TEM) assays

For TEM analysis under non-shear conditions, mo-DCs ($4\times10^5$ cells/ well) were labeled with carboxyfluorescein succinimidyl ester (CFSE, Thermo Fisher Scientific, Grand Island, NY, USA) and placed in a transwell chamber containing HUVEC monolayers (cultured on 8 μm pore membrane, Millipore); to induce HUVEC E-selectin and VCAM-1 expression, monolayers were exposed to TNFα (40 ng/mL) for 6 h ("stimulated" HUVECs). All assays were performed independent of chemokine addition, at 37°C for 12 h, and cell migration to the underside of transwell membrane was quantified by fluorescence microscopy. Controls consisted of evaluation of TEM on unstimulated HUVEC monolayers, and on stimulated HUVECs treated with function blocking anti-human E-selectin or isotype control mAb (20 μg/mL, 30 min). In some experiments, mo-DCs were treated with function blocking anti-VLA-4 mAb HP2/1 (Millipore, Billerica, MA, USA) or anti-LFA-1 mAb 24 (24) (20 μg/mL, 30 min) or pertussis toxin (PTX, Sigma) (250 ng/mL, 2 h).

For TEM analysis under hemodynamic fluid shear conditions, HUVECs were cultured on the underside of a transwell insert, stimulated with TNFα (as above), and placed into a flow chamber mounted on an inverted microscope, as previously described (20). Mo-DCs ($4\times10^6$ cells/mL) were perfused at 37°C over HUVECs at an initial shear rate of 0.5 dynes/$cm^2$ with subsequently increasing shear stress stepwise every 30 seconds until 7.5 dynes/ $cm^2$. The number of tethering and rolling mo-DCs, per $cm^2$ HUVEC area was quantified during each 30 second segment and the number of cells that became firmly adherent was recorded (20). The average rolling velocity, a measure of selectin binding strength, was evaluated at 2.0

dyn/cm$^2$, as the displacement of the centroid of the cell over 1 sec intervals. All experiments were performed and video-recorded for analysis.

### CS-1 fragment binding assay following E-selectin and hyaluronic acid engagement

Mo-DCs were placed in culture plates seeded with CHO-E or with mock transfectants (CHO-mock) or coated with E-Ig (10 μg/mL) or high molecular weight hyaluronic acid (HA, Sigma) (5 μg/μL). Mo-DCs, suspended in HBSS containing 2 mM $Ca^{2+}$, were placed onto the various plates for 30 min on a rocker platform (5–10 rpm). The cells were collected by vigorous pipetting, washed in HBSS without Ca/Mg, and then placed onto tissue culture plates previously coated with connecting segment-1 peptide (CS1) (Fibronectin-40 (Millipore, 10 μg/mL)). Mo-DCs were allowed to bind for 45 min at 37°C in RPMI-1640/10 mM HEPES/0.2% BSA. Plates were then washed, and adherent cells were identified by either crystal violet staining (absorbance 595 nm) or CFSE labeling (fluorescence signal).

### Western blotting and immunoprecipitation

Cell lysate proteins or immunoprecipitated proteins were resolved on reducing SDS-PAGE gels and electrotransferred to PVDF membranes. For immunoprecipitation, cell lysates were precleared with protein G-agarose (Invitrogen). For immunoprecipitation, precleared lysates were incubated with either anti-CD44 mAb (2C5) or anti-PSGL-1 mAb (clone KPL-1) or E-Ig chimera; for immunoprecipitation using E-Ig chimera, lysis buffer contained 2mM $Ca^{2+}$. Antibody or E-Ig immunoprecipitates were collected using protein G-agarose beads, which were washed with lysis buffer, pelleted and then resuspended in reducing sample buffer. The bead suspension was boiled, and supernatant (released protein) was subjected to SDS-PAGE, transferred to PVDF membrane, and blots were immunostained. E-Ig staining was done using a 3-step protocol (E-Ig immunostaining, followed by rat anti-mouse CD62E mAb (R&D Systems), then followed by horseradish peroxidise (HRP)-conjugated anti-rat IgG). Specificity for E-Ig binding was confirmed by loss of E-Ig reactivity in presence of EDTA and following sialidase treatment of cells (i.e., removal of sialic acid from $sLe^x$).

### Fucosyltransferase VI treatment

Cells were treated with 60 mU/mL fucosyltransferase-VI (FTVI (Warrior Therapeutics, Sudbury, MA), in HBSS containing 20 mM HEPES, 0.1% human serum albumin (HSA, Sigma) and 1 mM GDP-fucose (Carbosynth, Compton, UK) for 45 min at 37°C. Control consisted of cells treated with buffer containing all components except FTVI enzyme. The efficacy of the FTVI treatment was confirmed by evaluating for increased expression of E-selectin ligands as assessed by both flow cytometry and western blot analysis using E-Ig chimera as probe.

### Mice

Six to eight-week-old NOD/SCID IL-2Rγnull mice (NSG, Jackson Laboratories, Bar Harbor, ME USA) were housed and bred at the BWH animal facility. Mice were sacrificed by carbon dioxide inhalation followed by cervical dislocation. All mice were age and sex matched for each experiment. All animal experiments were conducted in accordance with

U.S. National Institutes of Health guidelines for care and use of animals under approval of the Institutional Animal Care and Use Committees of BWH (2016n000469).

### Bone marrow homing assay

Human mo-DCs were harvested and either FTVI- or buffer-treated as described above. Mo-DCs were then suspended in RPMI medium at $1\times10^7$ cells/mL and split into two groups for dye labeling, with either 10 μM CellTraceTM CFSE or CellTraceTM Far Red (Thermo Fisher Scientific, Grand Island, NY, USA), for 20 min at 37°C. Subsequently, cells were washed 3 times with ice-cold RPMI supplemented with 10% fetal bovine serum. Reciprocal mixtures of 1:1 (FTVI-treated DCs and buffer treated-DCs) were prepared for each dye combination. Recipient NSG mice were intravenously co-injected (retro-orbitally) with $2.5\times10^6$ FTVI-treated mo-DCs or $2.5\times10^6$ buffer-treated mo-DCs in a volume of 0.1 mL of PBS. After 24 h, both tibias and femurs were removed, and the bone marrow was flushed. The collected cell suspensions were strained, washed and erythrocytes were lysed in $NH_4Cl$ buffer. The presence of homed mo-DCs in bone marrow was assessed by flow cytometry of dye-labeled cells. The data collected were analyzed with FlowJo software version 10.0.5 (TreeStar, San Carlos, CA, USA). Fold change of FTVI-treated mo-DCs compared to buffer-treated mo-DCs was calculated for each mouse (6 mice, 3 mice for each dye combination).

### Statistical analysis

Data are expressed as the mean ± standard deviation (SD). Statistical significance was determined using the GraphPad PRISM software version 6.00 (San Diego, CA, USA). Differences between means were determined by one-way analysis of variance. Multiple comparisons were performed post-hoc by the Tukey *t* test. Statistical significance was defined as $P \leq 0.05$.

## Results

### CD14-S mo-DCs display higher TEM than PA-S mo-DCs in absence of input chemokine gradients

To assess whether monocyte enrichment methods affect endothelial adhesive interactions, we compared the ability of CD14-S and PA-S mo-DCs to execute TEM, in absence of applied chemokine gradients, on unstimulated HUVECs or HUVECs stimulated with TNFα to up-regulate E-selectin and VCAM-1 expression (25). On unstimulated HUVECs, only a small percentage of CD14-S or PA-S mo-DCs (1.25% (± 0.2%) or 1.28% (± 0.2%), respectively) executed TEM. While both types of mo-DCs have higher TEM on stimulated compared to unstimulated HUVECs, CD14-S mo-DCs undertake markedly more TEM on stimulated HUVECs compared to PA-S mo-DCs (Figure 1A). This augmented TEM was abrogated by function blocking antibodies against E-selectin and by sialidase treatment of mo-DCs, highlighting a key role for E-selectin receptor/ligand interactions in the extravasation process (Figure 1A). Moreover, the heightened TEM of CD14-S mo-DCs was blocked by function-blocking mAb to the VCAM-1 ligand VLA-4 (i.e., α4β1 or CD49d/CD29), but not to the ICAM-1 ligand LFA-1 (αLβ2, CD11a/CD18) (Figure 1A), indicating that the observed TEM on stimulated HUVEC requires engagement of both E-selectin/E-selectin ligands and VLA-4/VCAM-1. Furthermore, pretreatment with pertussis toxin

(PTX), a specific inhibitor of Gαi-dependent signaling, inhibited TEM of both types of mo-DC (Figure 1A), indicating that G-protein-mediated signaling is requisite for mo-DC transmigration.

In human mesenchymal stem cells and lymphoid cells (26–28), it has been reported that engagement of E-selectin ligands directly up-regulates VLA-4 integrin-mediated binding in the absence of chemokine input. We thus sought to examine whether β1 integrin activation occurs following engagement of E-selectin ligands on CD14-S and PA-S mo-DCs. To assess VLA-4 function, we tested mo-DC adhesiveness to CS-1 fibronectin fragment, binding to which depends on activation of VLA-4. Engagement of CD14-S mo-DCs on immobilized E-selectin significantly increased adhesiveness of these cells to CS-1 fibronectin fragment (Figure 1B). CS-1 adhesiveness was significantly reduced by function-blocking mAb against E-selectin, confirming the contribution of E-selectin engagement in priming VLA-4 binding to CS-1 (Figure 1B). However, engagement of PA-S mo-DCs on E-selectin did not induce significant mo-DC adherence to CS-1 fibronectin (Figure 1B), which was consistent with their reduced TEM ability on stimulated HUVECs. Staining with mAb directed to the activation epitope of VLA-4 β1-chain (CD29) was observed after engagement of CD14-S mo-DCs on immobilized E-selectin and was not observed on PA-S cells exposed to immobilized E-selectin, consistent with lack of fibronectin binding by PA-S cells (Figure 1C). Activation of the β2-integrin LFA-1 (CD11/CD18) after engagement on immobilized E-selectin was not observed on CD14-S mo-DCs (Figure 1D). Collectively, these data show that engagement of E-selectin ligands on human CD14-S mo-DCs, but not on PA-S mo-DCs, leads directly to activation of VLA-4 and subsequent transmigration.

## HCELL is expressed by CD14-S mo-DCs

To identify the molecular effectors of mo-DC TEM, we compared expression of E-selectin ligands and of VLA-4 in both CD14-S and PA-S mo-DCs. By flow cytometry, expression of VLA-4, PSGL-1, and CD44 was equivalent between CD14-S and PA-S mo-DCs (Figure 2A), and, though HECA-452 reactivity (i.e., $sLe^x$ expression) was similar on both types of mo-DCs, E-Ig reactivity was slightly higher in CD14-S mo-DC (Figure 2A). However, western blot analysis of reduced SDS-PAGE gels revealed pronounced differences in E-Ig-reactive bands between CD14-S and PA-S mo-DCs (Figure 2B). For both types of mo-DCs, E-Ig stained a ~120–130 kDa band, characteristic of the monomer chain of PSGL-1 (which natively exists as a disulfide-linked homodimer of ~240 kDa); the term “CLA” refers to the E-selectin-binding glycovariant of PSGL-1 (Figure 2B). E-selectin-reactive proteins (i.e., E-Ig immunoprecipitants) of CD14-S and PA-S mo-DCs showed equivalent reactivity on western blot with anti-PSGL-1 mAb (Figure 2C), thus confirming the expression of CLA by both types of mo-DCs. Importantly, only CD14-S mo-DCs showed an additional E-Ig reactive ~80–90 kDa band (Figure 2B), a migration pattern consistent with that of the CD44 glycoform HCELL. Consistently, CD44 immunoprecipitated from CD14-S mo-DCs, but not from PA-S mo-DCs, showed reactivity with E-Ig, confirming that the E-Ig reactive ~80–90 kDa protein on CD14-S mo-DCs is HCELL (Figure 2D). Moreover, in blot rolling assays, CD44 immunoprecipitated from CD14-S mo-DC lysates supported E-selectin-transfected Chinese hamster ovary (CHO) cells (CHO-E) rolling interactions under physiologic shear conditions (Figure 2E).

### Ligation of CD44 triggers β1-integrin activation in CD14-S mo-DCs

To assess the relative contribution(s) of HCELL to the augmented E-selectin-mediated TEM of CD14-S mo-DCs, we compared the effects of engagement of CD44/HCELL and PSGL-1/CLA on VLA-4 function. We examined whether the ligation of each of the pertinent scaffold proteins, CD44 and PSGL-1, to their canonical ligands, hyaluronic acid (HA) and P-selectin, respectively, alter VLA-4 binding activity. Notably, exposure of CD14-S mo-DCs to HA (Supplemental Figure S1A) consistently resulted in β1-integrin activation (Figure 3A), but exposure of PA-S mo-DCs to HA did not yield β1-integrin activation, nor did engagement of either CD14-S or PA-S mo-DCs with P-selectin (Figure 3A). Moreover, in CD14-S mo-DCs, but not PA-S mo-DCs, CD44 engagement with HA increased mo-DC adhesiveness to CS-1 fibronectin in a VLA-4-dependent manner (Figure 3B). These data highlight a predominant role of CD44 ligation in VLA-4 activation.

### TNFα-treatment boosts TEM of CD14-S mo-DCs

The inflammatory cytokine TNFα induces DC maturation (29), and is routinely used in clinical applications (30). We thus assessed whether TNFα treatment could affect mo-DC TEM ability. When treated with TNFα for 2 days (after 5 days of differentiation), both CD14-S and PA-S mo-DCs showed characteristic increased expression of MHC Class II antigens and the co-stimulatory molecule CD86. However, only CD14-S mo-DCs displayed increased transmigration on stimulated HUVEC (Figure 4A). TEM of CD14-S mo-DCs was abrogated by function-blocking anti-E-selectin mAb, by sialidase treatment of mo-DCs, by function-blocking anti-VLA-4 mAb and by PTX treatment of mo-DCs, confirming a role for both E-selectin receptor/ligand interactions and G-protein-signaling in driving VLA-4-dependent adhesive interactions (Figure 4A).

To determine whether the enhanced CD14-S mo-DC TEM following TNFα treatment could be secondary to changes in integrin levels, we measured the cell surface expression of the heterodimer chains of VLA-4 and LFA-1. While no significant increase was observed on cell surface expression of the CD29, CD18 or CD11a integrin subunits, surface expression of CD49d was considerably augmented after TNFα treatment (Figure 4B), which is in agreement with previous reports (31). TNFα-treated CD14-S mo-DCs also showed a significantly increased expression of the activation epitope of β1-integrin upon engagement on CHO-E cells and, commensurately, displayed increased VLA-4 binding to the CS-1 fibronectin fragment (Figure 4C). Altogether, these data indicate that TNFα induces VLA-4 expression on CD14-S mo-DCs and confirms a role for E-selectin receptor/ligand interactions in priming VLA-4 integrin activation in these cells.

### TNFα treatment of CD14-S mo-DCs sustains E-selectin ligand expression during culture

To assess whether the differences in TEM and integrin activation in CD14-S mo-DCs cultured in presence or absence of TNFα reflected differences in expression of E-selectin ligands, we performed flow cytometry, parallel plate-based assays, and western blot analysis to assess E-selectin binding of these cells. Following differentiation of monocytes into mo-DCs, there was no difference in flow cytometry profile of E-Ig staining between Day 0 CD14-S cells (Figure 2A) and those cells cultured for three days in absence (“untreated”) or presence of TNFα (“matured mo-DCs”) (Figures 5A). However, compared to untreated

CD14-S mo-DCs, TNFα-treated CD14-S mo-DCs showed markedly lower rolling velocity on stimulated HUVECs under hemodynamic fluid shear conditions (indicative of increased E-selectin avidity) (Figure 5B), and western blot analysis showed significantly greater E-Ig staining of lysates (Figure 5C). Specifically, compared with cells at start of culture (Day 0 cells), Day 3-cultured untreated mo-DCs showed significantly reduced levels of CLA and HCELL (i.e., E-Ig reactive bands at ~120–130 kDa and ~80–90 kDa, respectively), whereas TNFα-treated mo-DCs showed sustained E-Ig reactivity, with blot profile similar to that observed on Day 0 (Figure 5C). In contrast to CD14-S mo-DCs, the blot profile of E-Ig reactivity of PA-S mo-DCs was unchanged by TNFα treatment (Supplemental Figure S1B). Notably, though E-Ig staining patterns by western blot were markedly different, CD44 levels were only slighter higher on CD14-S mo-DCs between Day 0 and Day 3 of culture (Figure 5D), indicating that observed markedly increased HCELL expression (i.e., higher E-Ig reactivity) reflects increased content of $sLe^x$ on the CD44 scaffold and not changes in expression of the CD44 protein itself.

The E-selectin binding determinant $sLe^x$ is displayed on *O*-glycans in CLA(32) and on *N*-glycans in HCELL(33). To assess whether TNFα induces expression of enzymes critical to the biosynthesis of $sLe^x$ (11, 13, 34) (Figure 5E), we performed Real Time-PCR (RT-PCR) to analyze expression of the α(1,3)-fucosyltransferases (FTs) FTIV, FTVI and FTVII, and the α(2,3)-sialyltransferases (STs) ST3GalIII, ST3GalIV, and ST3GalVI, which add fucose and sialic acid, respectively, to lactosaminyl glycan precursors of $sLe^x$ (35). Moreover, we evaluated the expression of the core 2-synthase, C2GnT1, which forms the scaffold glycan for polylactosamine extension on *O*-glycans, and the enzymes ST3GalI and ST6GalNAcII, each which act on core 1 *O*-glycans and antagonize core 2 extensions (Figure 5E), thereby down-regulating *O*-glycan expression of $sLe^x$ (11, 36). We also analyzed the expression of Neu1 and Neu3 sialidases in mo-DCs (37), which are known to remove sialic acid moieties from $sLe^x$ (34). As shown in Figure 5F, TNFα-treated mo-DCs showed significantly more expression of FTVI, FTVII and ST3GalVI and less expression of ST3GalI and ST6GalNAcII, compared to that of untreated cells, with no differences in RNA transcripts encoding sialidases Neu1 and Neu3. Altogether, these changes in glycosyltransferase gene expression would serve to augment display of cell surface $sLe^x$ on both *O*- and *N*-glycans.

## FTVI treatment of CD14-S mo-DCs increases the expression of functional E-selectin ligands and increases transendothelial migration in vitro and bone marrow (BM) homing in vivo

HCELL is prominently expressed by human hematopoietic stem/progenitor cells, including the human hematopoietic progenitor cell line KG1a, and it is known to function as the principal bone marrow “homing receptor” in humans (38). Compared with KG1a cells, the levels of E-selectin ligands and of HCELL expressed by CD14-S mo-DCs are relatively modest (Figure 6A). We thus sought to determine whether stereoselective α(1,3)-exofucosylation using the α(1,3)-fucosyltransferase FTVI could boost DC surface expression of E-selectin ligands; notably, this enzyme is known to fucosylate sialylated type II lactosaminyl glycans on CD44 thus generating HCELL (27). Importantly, exofucosylation with FTVI is a rapid and non-toxic cell treatment (i.e., a 45 minute procedure, with no change in cell viability), it has only one cell effect (i.e., augmentation of $sLe^x$ display), it

reproducibly augments HCELL expression, and its incremental costs are not significant given the alternative of prolonged TNFα-culture of cells in presence of GM-CSF and IL-4. With FTVI treatment of mo-DCs at Day 5 of differentiation, we consistently observed a marked increase in E-Ig reactivity in both CLA and HCELL by western blot (Figure 6B), and increased transmigration (~2-fold more) compared to buffer-treated (BT) mo-DCs (Figure 6C). Notably, exofucosylation of PA-S mo-DCs also increased E-Ig binding, with increased reactivity at ~130 kDa (consistent with CLA) and *de novo* expression of a faint E-Ig-reactive ~80–90 kDa band (consistent with HCELL; Supplemental Figure S1C). However, PA-S mo-DCs treated with FTVI displayed no significant change in transmigration compared to BT mo-DCs (Supplemental Figure S1C).

To analyze the effect of FTVI treatment on E-selectin-dependent tethering/rolling interactions, we assessed binding of Day 5-differentiated CD14-S mo-DCs to unstimulated and TNFα-stimulated HUVECs under physiological shear stress conditions. For both BT and FTVI-treated CD14-S mo-DCs, there were no binding interactions observed on unstimulated HUVECs. On stimulated HUVECs, BT CD14-S mo-DCs exhibited a uniform but modest capacity to tether and roll, with cells transitioning to firm adherence under flow (Figure 6D). Notably, FTVI treatment of CD14-S mo-DCs led to a significant increase in the number of tethering/rolling and firmly adherent cells and markedly decreased rolling velocity compared to that of BT cells (Figures 6D and 6E), indicating increased adhesion to E-selectin. FTVI treatment did not alter the expression levels of CD44 or PSGL-1 or of other proteins involved in cell trafficking such as β1- and β2-integrins (Figure 6F), suggesting that the decreased rolling velocity of α(1,3)-exofucosylated mo-DCs was primarily due to increased levels of cell surface E-selectin ligands.

To assess whether FTVI-treatment would enhance mo-DC ability to migrate to E-selectin-bearing sites *in vivo*, we measured bone marrow accumulation of BT and FTVI-treated mo-DCs adoptively transferred into NSG mice. To this end, at 24 h post-intravenous injection, mouse bone marrow was harvested and analyzed by flow cytometry for the presence of mo-DCs. As shown in Figure 6G, FTVI-treatment of mo-DCs yielded significantly increased BM homing compared to that of BT cells.

## Discussion

The capacity to shape the tissue colonization capabilities of culture-expanded human DCs has immense implications for success of DC-based immunotherapeutics. Human DCs can be generated *in vitro* from human monocyte precursors (mo-DCs)(29) in sufficient numbers for clinical applications following CD14 immunomagnetic separation (CD14-S) and plastic adherence separation (PA-S) of blood monocytes (39). It has been reported that these different monocyte isolation methods may affect phenotypic proprieties of the generated DCs (4, 40). Yet, it is unknown whether different monocyte enrichment techniques could have subsequent effects on DC-endothelial interactions critical to extravasation. Accordingly, in this study, we examined DCs derived from both PA and CD14-S monocyte selection for their capability to undergo transendothelial migration (TEM) and evaluated the adhesion molecules mediating TEM for each of these mo-DC populations.

To compare E-selectin ligand expression in each mo-DC population, we performed both flow cytometry and western blot analysis using E-Ig as a probe. For assessment of E-selectin ligand expression, these techniques are complementary, but it is important to note that flow cytometry detects E-selectin binding to cell surface glycoproteins and glycolipids, while western blot detects E-selectin binding only among glycoproteins. Moreover, in general, western blot studies of E-Ig reactivity offer a better estimate of E-selectin binding capacity of cells under hemodynamic shear conditions, as glycoprotein selectin ligands are more potent effectors of selectin binding than are glycolipids (41). By flow cytometry, E-Ig reactivity was slightly higher in CD14-S mo-DCs compared to PA-S mo-DC, and, following treatment of mo-DCs with the potent protease bromelain, substantial E-Ig reactivity persisted indicating that mo-DCs express a significant amount of sialofucosylated structures on glycolipid scaffolds (supplemental Figure S1D). However, western blot revealed a striking difference in the profile of E-selectin ligands: while both mo-DC types showed robust staining of CLA (the glycovariant of PSGL-1), only CD14-S mo-DCs showed an E-Ig-reactive glycoprotein at a ~80–90 kDa band. Biochemical studies indicated that this second band represents HCELL, the specialized glycovariant of CD44 that binds E-selectin, providing first evidence that this structure can be found on human DCs (15, 33, 42, 43).

Our studies reveal that engagement of CD14-S mo-DCs with E-selectin leads to a remarkable increase in VLA-4-mediated adhesiveness to TNFα-stimulated HUVEC monolayers. Interestingly, exposure of mo-DCs to hyaluronic acid or to P-selectin, ligands specific to the protein scaffolds CD44 or PSGL-1, respectively, showed that ligation of CD44, but not PSGL-1, induced VLA-4 activation. These data indicate that E-selectin ligation of HCELL, and not CLA, drives VLA-4-mediated firm adherence and subsequent TEM of mo-DCs. More specifically, in contrast to the canonical multistep model of cell migration, whereby engagement of chemokine receptor(s) (step 2) is obligatory to achieve integrin activation (step 3), we observed that HCELL ligation by E-selectin alone triggers PTX-inhibitable endothelial transmigration, consistent with a G-protein-dependent inside-out stimulation of VLA-4 activity. The higher the E-selectin binding of the cells, the higher the “step 2” activation of VLA-4 adhesiveness, with no necessity of chemokine-mediated signaling. The extent to which the commensurate TEM is triggered by augmented endothelial firm adherence (step 3) versus augmented diapedesis itself (step 4) was not evaluated; but, it is suggested that this capacity of E-selectin to initiate mo-DC transmigration is due to the fact that $sLe^x$ binding determinants are expressed on the CD44 scaffold, thereby engendering E-selectin-mediated CD44 ligation. Though this CD44-dependent “step 2-chemokine bypass pathway” has been described in human mesenchymal stem cells following enforced HCELL expression by cell surface glycan engineering (26, 27), these results are the first to indicate that natively-expressed HCELL and VLA-4 can function in a bimolecular axis to drive transmigration of a human leukocyte.

TNFα is widely used to promote the maturation of DCs in immunotherapy (30). This pro-inflammatory cytokine characteristically increases the expression of E-selectin and VCAM-1 on endothelial cells (10, 44), but its effect on E-selectin ligand expression or on VLA-4 expression on mo-DCs was previously unknown. Our data show that TNFα preserves the expression of HCELL on culture-expanded CD14-S mo-DCs, which otherwise undergoes time-dependent decay following differentiation of DC from monocytes. TNFα

also increases expression of VLA-4, and, therefore, the combined effect on HCELL and VLA-4 expression would license augmented β1-integrin activation and consequent TEM on endothelial beds expressing both E-selectin and VCAM-1. Commensurate with its observed effects on HCELL induction, and consistent with prior reports of TNFα effects on glycosyltransferases (13, 45), we observed significant changes in expression of glycosyltransferase genes with exposure of CD14-S mo-DCs to TNFα: as compared to untreated CD14-S mo-DCs, TNFα-treated DCs express lower levels of transcripts encoding ST3GalI and ST6GalNAcII, and higher levels of that of C2GnT1; this pattern would promote the expression of core 2 glycan structures that are requisite for elaboration of the CLA glycoform of PSGL-1. In addition, TNFα treatment upregulates expression of the fucosyltransferases FTVI and FTVII and of the sialyltransferase ST3GalVI, which, collectively, heighten requisite α(1,3)-fucosylation and α(2,3)-sialylation of lactosamine chains to create $sLe^x$ (6). This pattern of glycosyltransferase gene expression would serve to sustain HCELL expression, as observed in TNFα–treated CD14-S mo-DCs.

Apart from cytokine effects on expression of Golgi glycosyltransferases, cell surface $sLe^x$ expression can be modulated via stereospecific exoglycosylation (26, 46). FTVI places fucose in α(1,3)-linkage to an acceptor *N*-acetylglucosamine located specifically within a terminal α(2,3)-sialylated type 2 lactosamine unit (NeuAcα2-3Galβ1-4GlcNAcβ1-R, Figure 5E). Here, we found that FTVI treatment of CD14-S mo-DCs increased both HCELL and CLA expression and markedly enhances TEM. In contrast, FTVI treatment of PA-S mo-DCs did not augment HCELL expression, and, despite increased CLA expression, TEM was unchanged after FTVI treatment of PA-S mo-DCs. Furthermore, FTVI treatment also improved mo-DC homing to bone marrow after intravenous adoptive transfer into mice. These findings indicate that DC glycoengineering to increase HCELL expression augments TEM and E-selectin-bearing tissue tropism of mo-DCs, whereas enforced CLA expression alone does not, therefore highlighting a key role for HCELL in licensing mo-DC TEM.

The results of our studies offer new insights into the role of CD44 in DC biology. Our findings that human DCs express HCELL have important implications for elucidating the molecular basis of DC migration, and for optimizing DC tissue delivery in adoptive cell therapeutics. The observation that HCELL is expressed by CD14-S mo-DCs but not by PA-S mo-DCs indicates that *in vitro* monocyte isolation/DC generation methods impact expression of E-selectin ligands and mo-DC transmigration. While TNFα is well-known to upregulate expression of E-selectin and VCAM-1 on endothelial cells, the data here indicate that TNFα also preserves the expression of E-selectin ligands on culture-expanded mo-DCs, thereby priming E-selectin- and VLA-4-dependent transmigration of mo-DCs (see model represented in Figure S2). Our findings thus offer a unifying perspective on the role of TNFα in promoting tissue recruitment of DCs, and altogether, yield novel insights into a how a CD44-based non-canonical TEM pathway could be exploited to help realize the enormous clinical potential of DC-based therapeutics.

## Supplementary Material

Refer to Web version on PubMed Central for supplementary material.

## Acknowledgments

We thank Cristina Silvescu, Brad Dykstra, Jack Lee and Conor Donnelly for technical assistance and helpful discussions.

**Financial support:** This work was supported by the National Institutes of Health (NIH), in particular, the National Heart Lung Blood Institute (NHLBI) Program of Excellence in Glycosciences (PEG) grant PO1-HL107146 (to R.S.), and the National Cancer Institute grant RO1 CA121335 (to R.S.). Funding was also provided by the Fulbright Commission (2012/2013 to P.V.), the European Molecular Biology Organization (EMBO, YIP project 2402 to P.V.) and the Portuguese Foundation for Science and Technology (SFRH/BD/81860/2011 to M.S.).

## Abbreviations list

| | |
|---|---|
| **BT** | Buffer-Treated |
| **CD14-S** | CD14-selection |
| **CFSE** | Carboxyfluorescein Succinimidyl Ester |
| **CHO** | Chinese Hamster Ovary |
| **CLA** | Cutaneous Lymphocyte Antigen |
| **DC** | Dendritic Cell |
| **E-Ig** | mouse E-selectin-human Fc Ig chimera |
| **FT** | Fucosyltransferase |
| **HA** | Hyaluronic Acid |
| **HCELL** | Hematopoietic Cell E-selectin/ L-selectin Ligand |
| **HEV** | High Endothelial Venule |
| **HUVEC** | Human Umbilical Vein Endothelial Cell |
| **IL** | Interleukin |
| **Mo-DC** | Monocyte-derived Dendritic Cells |
| **PA-S** | Plastic Adherence-Selection |
| **PBMC** | Peripheral Blood Mononuclear Cells |
| **PSGL-1** | P-selectin Glycoprotein Ligand-1 |
| **RT-PCR** | Real Time-PCR |
| **sLe$^X$** | Sialyl Lewis X |
| **ST** | Sialyltransferase |
| **TEM** | Transendothelial Migration |
| **TNFα** | Tumor Necrosis Factor-α |

**VCAM-1** Vascular Cell Adhesion Molecule-1

**VLA-4** Very Late Antigen-4

## References


1. Steinman RM. Dendritic cells in vivo: a key target for a new vaccine science. Immunity. 2008; 29:319–324. [PubMed: 18799140]
2. Silva Z, Konstantopoulos K, Videira PA. The role of sugars in dendritic cell trafficking. Annals of biomedical engineering. 2012; 40:777–789. [PubMed: 22045510]
3. Robert C, Klein C, Cheng G, Kogan A, Mulligan RC, von Andrian UH, Kupper TS. Gene therapy to target dendritic cells from blood to lymph nodes. Gene therapy. 2003; 10:1479–1486. [PubMed: 12900763]
4. De Vries IJ, Krooshoop DJ, Scharenborg NM, Lesterhuis WJ, Diepstra JH, Van Muijen GN, Strijk SP, Ruers TJ, Boerman OC, Oyen WJ, Adema GJ, Punt CJ, Figdor CG. Effective migration of antigen-pulsed dendritic cells to lymph nodes in melanoma patients is determined by their maturation state. Cancer research. 2003; 63:12–17. [PubMed: 12517769]
5. Ferguson PM, Slocombe A, Tilley RD, Hermans IF. Using magnetic resonance imaging to evaluate dendritic cell-based vaccination. PLoS One. 2013; 8:e65318–e65330. [PubMed: 23734246]
6. Morse MA, Coleman RE, Akabani G, Niehaus N, Coleman D, Lyerly HK. Migration of human dendritic cells after injection in patients with metastatic malignancies. Cancer research. 1999; 59:56–58. [PubMed: 9892184]
7. Sackstein R. The lymphocyte homing receptors: gatekeepers of the multistep paradigm. Current opinion in hematology. 2005; 12:444–450. [PubMed: 16217160]
8. Schweitzer KM, Dräger AM, van der Valk P, Thijsen SF, Zevenbergen A, Theijsmeijer AP, van der Schoot CE, Langenhuijsen MM. Constitutive expression of E-selectin and vascular cell adhesion molecule-1 on endothelial cells of hematopoietic tissues. Am J Pathol. 1996; 148:165–175. [PubMed: 8546203]
9. Weninger W, Ulfman LH, Cheng G, Souchkova N, Quackenbush EJ, Lowe JB, von Andrian UH. Specialized contributions by alpha(1,3)-fucosyltransferase-IV and FucT-VII during leukocyte rolling in dermal microvessels. Immunity. 2000; 12:665–676. [PubMed: 10894166]
10. Yao L, Setiadi H, Xia L, Laszik Z, Taylor FB, McEver RP. Divergent inducible expression of P-selectin and E-selectin in mice and primates. Blood. 1999; 94:3820–3828. [PubMed: 10572097]
11. Julien S, Grimshaw MJ, Sutton-Smith M, Coleman J, Morris HR, Dell A, Taylor-Papadimitriou J, Burchell JM. Sialyl-Lewis(x) on P-selectin glycoprotein ligand-1 is regulated during differentiation and maturation of dendritic cells: a mechanism involving the glycosyltransferases C2GnT1 and ST3Gal I. Journal of immunology (Baltimore, Md.: 1950). 2007; 179:5701–5710.
12. Kieffer JD, Fuhlbrigge RC, Armerding D, Robert C, Ferenczi K, Camphausen RT, Kupper TS. Neutrophils, monocytes, and dendritic cells express the same specialized form of PSGL-1 as do skin-homing memory T cells: cutaneous lymphocyte antigen. Biochemical and biophysical research communications. 2001; 285:577–587. [PubMed: 11453631]
13. Silva Z, Tong Z, Guadalupe Cabral M, Martins C, Castro R, Reis C, Trindade H, Konstantopoulos K, Videira PA. Sialyl Lewis(x)-dependent binding of human monocyte-derived dendritic cells to selectins. Biochemical and Biophysical Research Communications. 2011; 409:459–464. [PubMed: 21596017]
14. Sackstein R. The bone marrow is akin to skin: HCELL and the biology of hematopoietic stem cell homing. The Journal of investigative dermatology. 2004; 122:1061–1069. [PubMed: 15140204]
15. Dimitroff CJ, Lee JY, Fuhlbrigge RC, Sackstein R. A distinct glycoform of CD44 is an L-selectin ligand on human hematopoietic cells. Proceedings of the National Academy of Sciences of the United States of America. 2000; 97:13841–13846. [PubMed: 11095749]
16. Hegde VL, Singh NP, Nagarkatti PS, Nagarkatti M. CD44 mobilization in allogeneic dendritic cell-T cell immunological synapse plays a key role in T cell activation. J Leukoc Biol. 2008; 84:134–142. [PubMed: 18388297]

17. Weiss JM, Sleeman J, Renkl AC, Dittmar H, Termeer CC, Taxis S, Howells N, Hofmann M, Kohler G, Schopf E, Ponta H, Herrlich P, Simon JC. An essential role for CD44 variant isoforms in epidermal Langerhans cell and blood dendritic cell function. The Journal of cell biology. 1997; 137:1137–1147. [PubMed: 9166413]
18. Cabral MG, Silva Z, Ligeiro D, Seixas E, Crespo H, Carrascal MA, Silva M, Piteira AR, Paixão P, Lau JT, Videira PA. The phagocytic capacity and immunological potency of human dendritic cells is improved by α2,6-sialic acid deficiency. Immunology. 2013; 138:235–245. [PubMed: 23113614]
19. Crespo HJ, Cabral MG, Teixeira AV, Lau JTY, Trindade H, Videira PA. Effect of sialic acid loss on dendritic cell maturation. Immunology. 2009; 128:e621–e631. [PubMed: 19740323]
20. Lee JY, Buzney CD, Poznansky MC, Sackstein R. Dynamic alterations in chemokine gradients induce transendothelial shuttling of human T cells under physiologic shear conditions. Journal of leukocyte biology. 2009; 86:1285–1294. [PubMed: 19797295]
21. Spandidos A, Wang X, Wang H, Seed B. PrimerBank: a resource of human and mouse PCR primer pairs for gene expression detection and quantification. Nucleic Acids Res. 2010; 38:D792–799. [PubMed: 19906719]
22. Meijerink J, Mandigers C, van de Locht L, Tonnissen E, Goodsaid F, Raemaekers J. A novel method to compensate for different amplification efficiencies between patient DNA samples in quantitative real-time PCR. The Journal of molecular diagnostics : JMD. 2001; 3:55–61. [PubMed: 11333300]
23. Carrascal MA, Severino PF, Guadalupe Cabral M, Silva M, Ferreira JA, Calais F, Quinto H, Pen C, Ligeiro D, Santos LL, Dall'Olio F, Videira PA. Sialyl Tn-expressing bladder cancer cells induce a tolerogenic phenotype in innate and adaptive immune cells. Molecular oncology. 2014; 8:753–765. [PubMed: 24656965]
24. Dransfield I, Cabañas C, Craig A, Hogg N. Divalent cation regulation of the function of the leukocyte integrin LFA-1. J Cell Biol. 1992; 116:219–226. [PubMed: 1346139]
25. Mackay F, Loetscher H, Stueber D, Gehr G, Lesslauer W. Tumor necrosis factor alpha (TNF-alpha)-induced cell adhesion to human endothelial cells is under dominant control of one TNF receptor type, TNF-R55. J Exp Med. 1993; 177:1277–1286. [PubMed: 8386742]
26. Thankamony SP, Sackstein R. Enforced hematopoietic cell E- and L-selectin ligand (HCELL) expression primes transendothelial migration of human mesenchymal stem cells. Proceedings of the National Academy of Sciences of the United States of America. 2011; 108:2258–2263. [PubMed: 21257905]
27. Sackstein R, Merzaban JS, Cain DW, Dagia NM, Spencer JA, Lin CP, Wohlgemuth R. Ex vivo glycan engineering of CD44 programs human multipotent mesenchymal stromal cell trafficking to bone. Nature medicine. 2008; 14:181–187.
28. Catalina MD, Estess P, Siegelman MH. Selective requirements for leukocyte adhesion molecules in models of acute and chronic cutaneous inflammation: participation of E- and P- but not L-selectin. Blood. 1999; 93:580–589. [PubMed: 9885219]
29. Sallusto F, Lanzavecchia A. Efficient presentation of soluble antigen by cultured human dendritic cells is maintained by granulocyte/macrophage colony-stimulating factor plus interleukin 4 and downregulated by tumor necrosis factor alpha. J Exp Med. 1994; 179:1109–1118. [PubMed: 8145033]
30. Rosenblatt J, Wu Z, Vasir B, Zarwan C, Stone R, Mills H, Friedman T, Konstantinopoulos PA, Spentzos D, Ghebremichael M, Stevenson K, Neuberg D, Levine JD, Joyce R, Tzachanis D, Boussiotis V, Kufe D, Avigan D. Generation of tumor-specific T lymphocytes using dendritic cell/tumor fusions and anti-CD3/CD28. J Immunother. 2010; 33:155–166. [PubMed: 20145548]
31. Puig-Kröger A, Sanz-Rodríguez F, Longo N, Sánchez-Mateos P, Botella L, Teixidó J, Bernabéu C, Corbí AL. Maturation-Dependent Expression and Function of the CD49d Integrin on Monocyte-Derived Human Dendritic Cells. J Immunol. 2000; 165:4338–4345. [PubMed: 11035069]
32. Yago T, Fu J, McDaniel JM, Miner JJ, McEver RP, Xia L. Core 1-derived O-glycans are essential E-selectin ligands on neutrophils. Proceedings of the National Academy of Sciences of the United States of America. 2010; 107:9204–9209. [PubMed: 20439727]

33. Sackstein R, Dimitroff CJ. A hematopoietic cell L-selectin ligand that is distinct from PSGL-1 and displays N-glycan-dependent binding activity. Blood. 2000; 96:2765–2774. [PubMed: 11023510]
34. Gadhoum SZ, Sackstein R. CD15 expression in human myeloid cell differentiation is regulated by sialidase activity. Nature chemical biology. 2008; 4:751–757. [PubMed: 18953356]
35. Sperandio M. Selectins and glycosyltransferases in leukocyte rolling in vivo. The FEBS journal. 2006; 273:4377–4389. [PubMed: 16956372]
36. Lo CY, Antonopoulos A, Gupta R, Qu J, Dell A, Haslam SM, Neelamegham S. Competition between core-2 GlcNAc-transferase and ST6GalNAc-transferase regulates the synthesis of the leukocyte selectin ligand on human P-selectin glycoprotein ligand-1. The Journal of biological chemistry. 2013; 288:13974–13987. [PubMed: 23548905]
37. Stamatos NM, Carubelli I, van de Vlekkert D, Bonten EJ, Papini N, Feng C, Venerando B, d'Azzo A, Cross AS, Wang LX, Gomatos PJ. LPS-induced cytokine production in human dendritic cells is regulated by sialidase activity. Journal of leukocyte biology. 2010; 88:1227–1239. [PubMed: 20826611]
38. Merzaban JS, Burdick MM, Gadhoum SZ, Dagia NM, Chu JT, Fuhlbrigge RC, Sackstein R. Analysis of glycoprotein E-selectin ligands on human and mouse marrow cells enriched for hematopoietic stem/progenitor cells. Blood. 2011; 118:1774–1783. [PubMed: 21659548]
39. Delirezh N, Shojaeefar E, Parvin P, Asadi B. Comparison the effects of two monocyte isolation methods, plastic adherence and magnetic activated cell sorting methods, on phagocytic activity of generated dendritic cells. Cell J. 2013; 15:218–223. [PubMed: 24027662]
40. Elkord E, Williams PE, Kynaston H, Rowbottom AW. Human monocyte isolation methods influence cytokine production from in vitro generated dendritic cells. Immunology. 2005; 114:204–212. [PubMed: 15667565]
41. Sackstein R. Engineering cellular trafficking via glycosyltransferase-programmed stereosubstitution. Ann N Y Acad Sci. 2012; 1253:193–200. [PubMed: 22352800]
42. Burdick MM, Chu JT, Godar S, Sackstein R. HCELL is the major E- and L-selectin ligand expressed on LS174T colon carcinoma cells. The Journal of biological chemistry. 2006; 281:13899–13905. [PubMed: 16565092]
43. Silva M, Fung RKF, Donnelly CB, Videira PA, Sackstein R. Cell-Specific Variation in E-Selectin Ligand Expression among Human Peripheral Blood Mononuclear Cells: Implications for Immunosurveillance and Pathobiology. Journal of immunology. 2017; 198:3576–3587.
44. McEver RP. Selectins: lectins that initiate cell adhesion under flow. Current opinion in cell biology. 2002; 14:581–586. [PubMed: 12231353]
45. Videira PA, Amado IF, Crespo HJ, Alguero MC, Dall'Olio F, Cabral MG, Trindade H. Surface alpha 2–3- and alpha 2–6-sialylation of human monocytes and derived dendritic cells and its influence on endocytosis. Glycoconjugate Journal. 2008; 25:259–268. [PubMed: 18080182]
46. Sasaki K, Kurata K, Funayama K, Nagata M, Watanabe E, Ohta S, Hanai N, Nishi T. Expression cloning of a novel alpha 1,3-fucosyltransferase that is involved in biosynthesis of the sialyl Lewis x carbohydrate determinants in leukocytes. The Journal of biological chemistry. 1994; 269:14730–14737. [PubMed: 8182079]
47. Sackstein R. Glycosyltransferase-programmed stereosubstitution (GPS) to create HCELL: engineering a roadmap for cell migration. Immunol Rev. 2009; 230:51–74. [PubMed: 19594629]

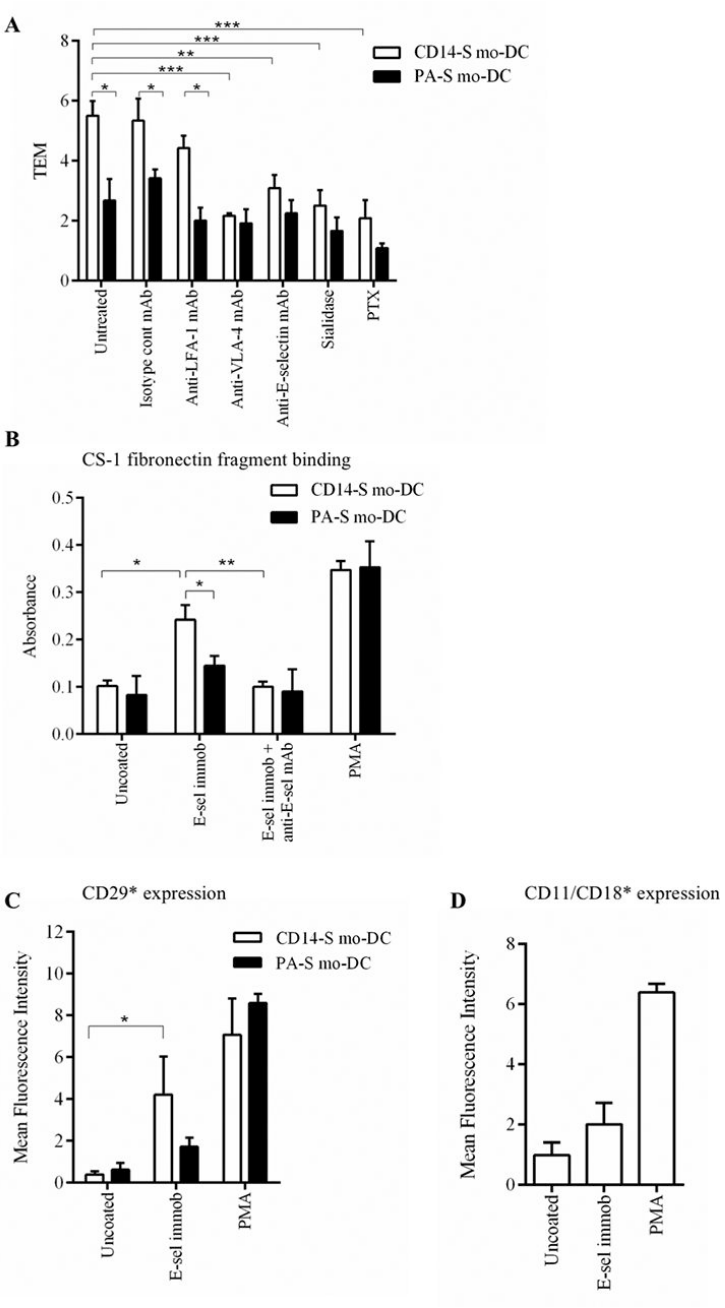


**Figure 1. Transendothelial migration of mo-DCs, in absence of chemokine, is dependent on engagement of E-selectin ligands and VLA-4**

**(A)** *Transendothelial migration (TEM) assay of CD14-S and PA-S mo-DCs on HUVEC monolayers*. The relative TEM value is the ratio of mo-DCs transmigrated on TNFα-stimulated HUVECs compared with mo-DCs transmigrated on non-stimulated HUVECs and in the absence of chemokines. TEM was assessed using mo-DCs (untreated), mo-DCs preincubated with isotype control or with function blocking anti-LFA-1 mAb or with function blocking anti-VLA-4 mAb, HUVECs preincubated with function blocking anti-E-selectin mAb, and mo-DCs treated with sialidase or pertussis toxin (PTX). **(B)** *Adhesiveness to CS-1 fibronectin fragment of CD14-S or PA-S mo-DCs.* Cells were first incubated on

uncoated or E-selectin-coated plates and then tested for binding to CS-1 peptide coated plates. Mo-DCs were stained with crystal violet and adherence was quantified by measuring light absorbance at 595 nm. Function blocking anti-E-selectin mAb was used as negative control and PMA treatment used as a positive control. **(C)** *Flow cytometry analysis of activated β1-integrin expression by CD14-S and PA-S mo-DCs*. Mo-DCs were incubated on uncoated plates or on E-selectin-coated plates, or cells were stimulated with PMA, and then stained with mAb HUTS-21 that identifies an activation-dependent epitope of β1-integrin (CD29*). Graph values represent the mean fluorescence intensity of HUTS-21 staining (n= 3, mean ± SD) subtracted from the values obtained using isotype control. **(D)** *E-selectin ligand engagement on CD14-S mo-DCs does not lead to direct LFA-1 activation*. Mo-DCs were incubated on uncoated or on E-selectin coated plates, or stimulated with PMA, and then stained with mAb 24 that recognizes an activation-dependent epitope of CD11/CD18 β2-integrin (CD11/CD18*). Graph values represent the mean fluorescence intensity of mAb 24 staining (n= 3, mean ± SD), subtracted from the values obtained using isotype control.

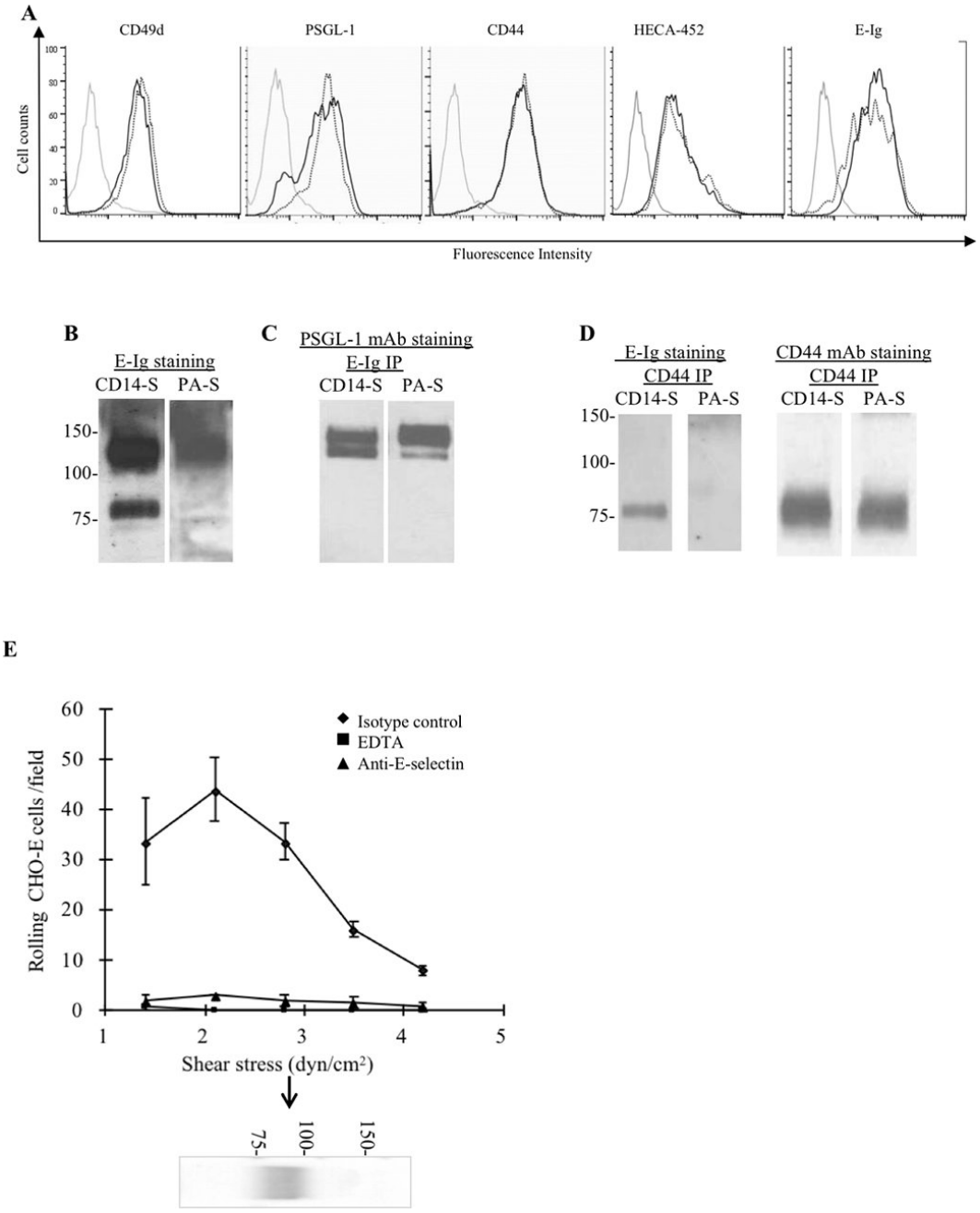


**Figure 2. Analysis of VLA-4 and E-selectin ligand expression on mo-DCs**

**(A)** *Representative flow cytometry analysis of mo-DCs staining using mAbs to CD49d (VLA-4), PSGL-1 and CD44, and HECA-452 mAb and E-Ig.* Grey lines represent isotype control (or, for E-Ig, staining in the absence of $Ca^{2+}$), dotted black line represents PA-S mo-DCs and solid black lines are CD14-S mo-DCs. **(B–D)** *Analysis of glycoprotein E-selectin ligands expressed by mo-DCs:* **(B)** Equivalent amounts of cell lysates of CD14-S and PA-S mo-DCs were resolved by SDS-PAGE electrophoresis, and immunoblotted with E-Ig chimera. Two E-selectin-reactive bands were visible in lysates of CD14-S mo-DCs (~130 kDa and ~80 kDa), whereas only one band (~130 kDa) was reactive on PA-S mo-DCs. **(C)**

Equivalent amounts of cell lysates of CD14-S and PA-S mo-DCs were immunoprecipitated with E-Ig, and immunoprecipitates were then electrophoresed and immunoblotted with anti-PSGL-1 mAb. **(D)** CD44 immunoprecipitates (CD44 IP) from equivalent amounts of cell lysates of CD14-S and PA-S mo-DCs were immunoblotted with E-Ig chimera or anti-CD44 mAb. **(E)** *Blot rolling assay of CD44 immunoprecipated from CD14-S mo-DCs*. CD44 immunoprecipitates were resolved by SDS-PAGE, blotted and stained with anti-CD44 mAb (blot below the graph). E-selectin-transfected CHO cells (CHO-E) were perfused over blots at 1.4 dyn/cm$^2$ and then shear stress was increased to 4.2 dynes/cm$^2$. E-selectin-dependent tethering and rolling was observed at the CD44 band (arrow). Assays were performed in the presence or absence of 5 mM EDTA, or following preincubation of CHO-E with isotype control mAb or function blocking anti-human E-selectin mAb (clone 68-5H11).

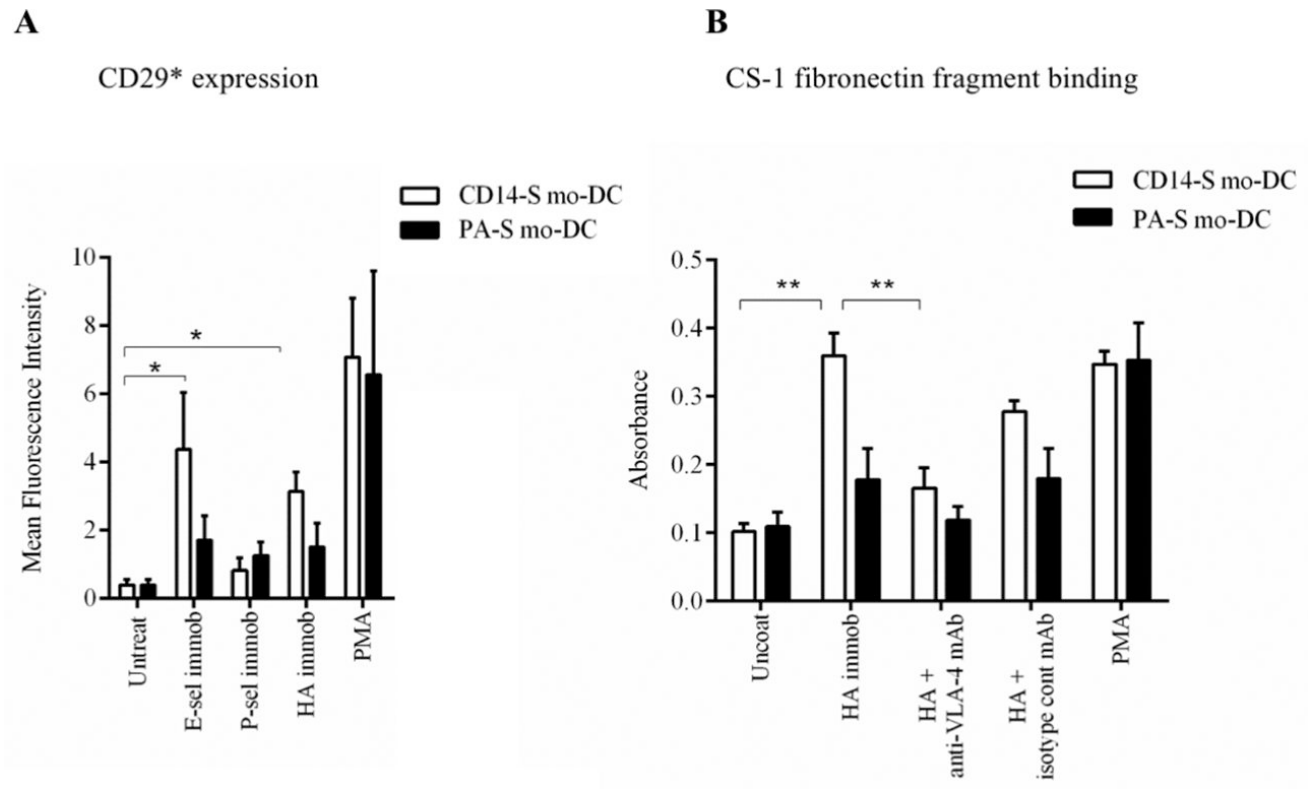


**Figure 3. VLA-4 binding activity is triggered by engagement of CD44 on CD14-S mo-DCs**

**(A)** *Flow cytometry analysis of activated β1-integrin expression*. Expression of the activation-dependent epitope of CD29 (HUTS-21) was assessed on CD14-S mo-DCs (white bars) and PA-S mo-DCs (black bars) incubated on plates coated with either E-selectin, P-selectin, or HA, or stimulated with PMA. Graph values represent the mean fluorescence intensity of HUTS-21 mAb staining (CD29*) of mo-DCs (n= 3, mean ± SD). **(B)** *Adhesion of CD14-S and PA-S mo-DCs to CS-1 fibronectin fragment*. Mo-DCs were incubated on uncoated plates or plates coated with HA, and then collected for analysis of binding to CS-1 peptide coated on plates. Integrin activation by treatment with PMA was used as positive control; the numbers of CS-1-adherent cells were quantified by light absorbance (595 nm) following crystal violet staining. As shown in the Figure, binding to HA by CD14-S mo-DCs, but not by PA-S mo-DCs, induced VLA-4 adhesion to CS-1 peptide, which was abrogated by treatment with anti-VLA-4 blocking mAb (HP2/1). Values are means ± SD (n= 3). Statistically significant differences ($P \leq 0.05$) related to HA engagement are indicated by brackets and asterisks.

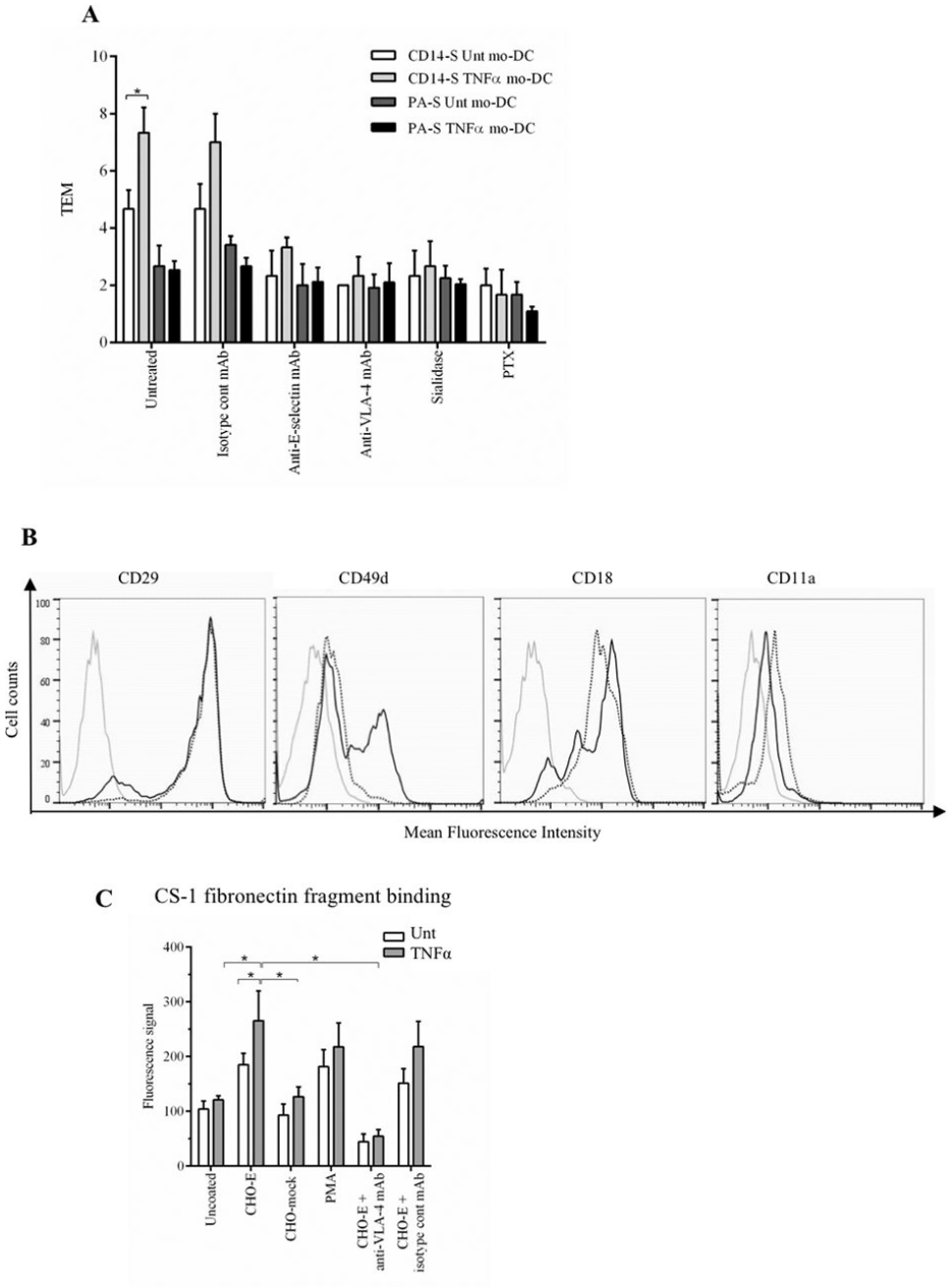


**Figure 4. TNFα-treatment of mo-DCs affects TEM and VLA-4 activity**

**(A)** *Transendothelial migration (TEM) assay of untreated (Unt) and TNFα-treated CD14-S and PA-S mo-DCs*. Both CD14-S and PA-S mo-DCs were left untreated or treated with TNFα for 2 days (after 5 days of differentiation). The relative TEM value was calculated as the ratio of transmigrated cells on TNFα-stimulated HUVECs compared with cells transmigrated on non-stimulated HUVECs. TEM values were analyzed for mo-DCs preincubated with isotype mAb, for HUVECs preincubated with function blocking anti-E-selectin mAb clone 68-5H1, for mo-DCs preincubated with function blocking anti-VLA-4 mAb HP2/1, and for mo-DCs treated with sialidase or PTX. **(B)** *Flow cytometry analysis of*

*cell surface expression of integrins VLA-4 and LFA-1 on CD14-S mo-DCs*. Histograms show the staining in untreated (dotted black line) and TNFα-treated (solid black line) mo-DCs. Grey lines represent isotype control. **(C)** *Analysis of CD14-S mo-DCs binding to CS-1 fibronectin fragment*. Adhesion of untreated (Unt) or TNFα-treated CD14-S mo-DCs (TNFα) to CS-1 peptide was assessed following incubation of mo-DCs on plates containing monolayers of E-selectin-transfected CHO cells (CHO-E), mock transfected CHO (CHO-mock), or plates containing no CHO cells (uncoated). After incubation, cells were collected for binding to CS-1 peptide coated on plates. The number of CS-1-adherent cells was quantified by light absorbance (595 nm) following crystal violet staining. Cells activated with PMA (positive control) bound avidly to CS-1, and preincubation of cells on CHO-E markedly augmented binding to CS-1. Incubation with anti-VLA-4 blocking antibody (HP2/1) for the last 15 min of CHO-E engagement (CHO-E+anti-VLA-4 mAb) abrogated binding to CS-1. Values are mean ± SD (minimum of n=4). Statistically significant differences ($P \leq 0.05$) related to CHO-E engagement are indicated by brackets and asterisks.

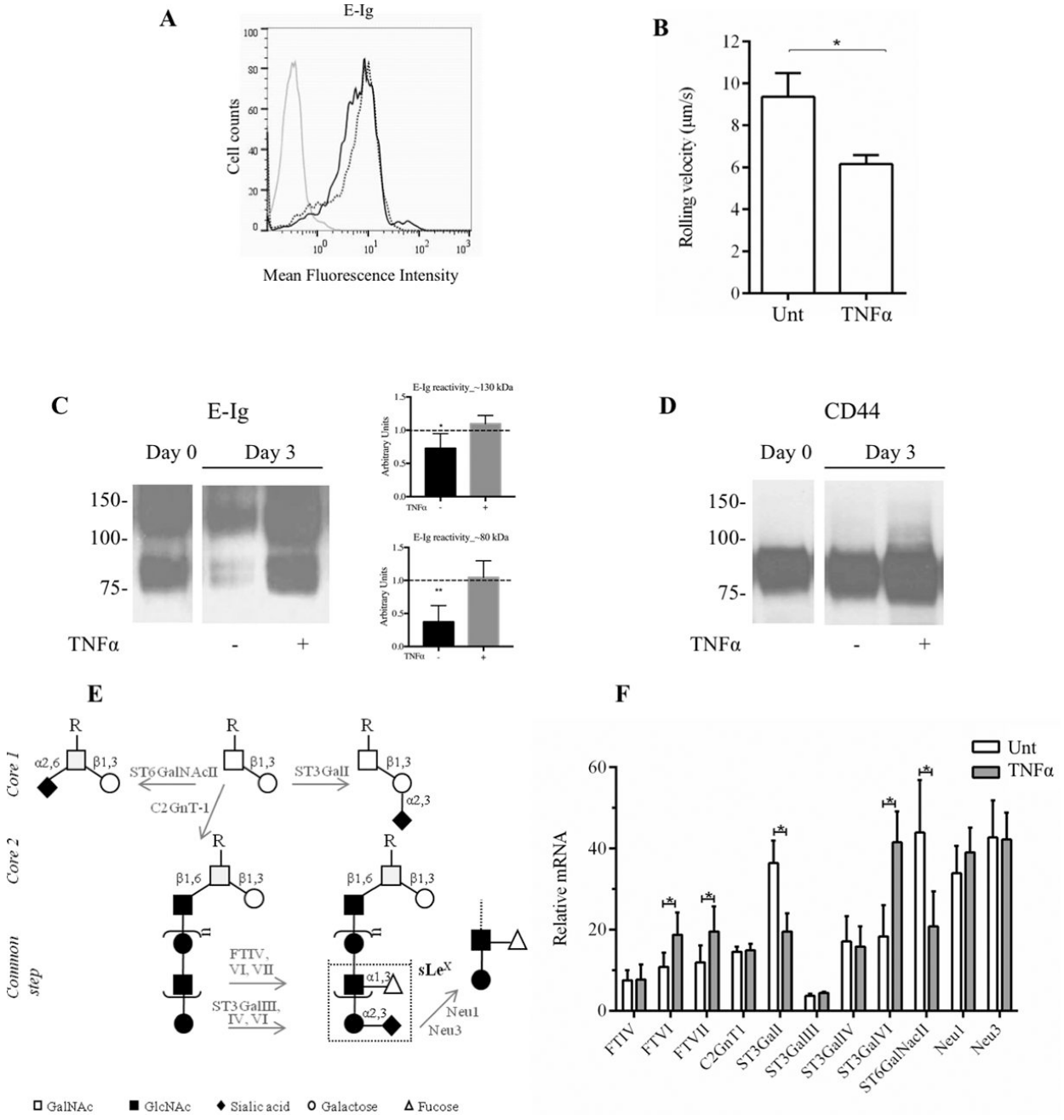


**Figure 5. E-selectin ligand expression on cultured human CD14-S mo-DCs is preserved by TNFα treatment**

**(A)** *Flow cytometry analysis of E-Ig reactivity on CD14-S mo-DCs*. Representative histograms of E-Ig staining of untreated mo-DCs (dotted black line) and mo-DCs treated with TNFα (solid black line) collected after 3 days of culture. Grey line represents E-Ig staining in absence of $Ca^{2+}$. **(B)** *Rolling adhesive interactions on TNFα-stimulated HUVECs of cultured CD14-S mo-DCs untreated (Unt) or treated with TNFα (TNFα) for 3 days*. Rolling velocities were measured at shear stress of 2.0 dyn/cm$^2$. The velocity was calculated by measuring the displacement of the centroid of the cell over 1 sec.; lower rolling velocity of TNFα mo-DCs indicates higher avidity to E-selectin. **(C)** *Western blot*

*analysis of E-Ig reactivity of whole cell lysates of CD14-S mo-DCs*. Cells were left untreated (−) or treated (+) with TNFα (at Day 0) and collected at Day 3 after treatment. Representative western blot analysis (left) and the average quantifications of E-Ig reactivity obtained by densitometric analysis of three independent experiments (right) show that lysates obtained from TNFα-treated mo-DCs display higher E-Ig reactivity at bands at ~130 kDa and ~80 kDa, than those obtained from untreated DCs. Values are shown in arbitrary density units as the density ratio of the ~130 kDa (Top plot) and ~80 kDa (Bottom plot) bands obtained from DCs collected at Day 3 in relation to those obtained from DCs collected at Day 0. Statistically significant differences ($P \leq 0.05$) are indicated by asterisks. **(D)** *Western blot analysis of CD44 expression of CD14-S mo-DCs*. Cells were collected at Day 0 and Day 3 with (+) or without (−) TNFα treatment. As shown in the figure, TNFα treatment sustains the expression of HCELL in vitro. **(E)** *Schematic of $sLe^X$ biosynthesis on N- and O-glycans*. Enzymes that were analyzed in this study are indicated in grey next to the arrows: core 2-synthase (C2GnT1), sialyltransferases (ST3GalI, ST3GalIII, ST3GalIV and ST3GalVI, ST6GalNAcII), fucosyltransferases (FTIV, VI and VII), and sialidases (Neu1, Neu3). **(F)** *Real-time PCR analysis showing relative expression of selected genes*. The relative mRNA level was computed as the permillage fraction (‰, i.e., the proportion of target mRNA per thousand of the reference *GAPDH* mRNA expression) of mo-DCs treated for 3 days with TNFα (grey bars) or left untreated (white bars). Values are means ± SD (n= 3). Statistical significant differences ($P \leq 0.05$) are indicated by asterisks.

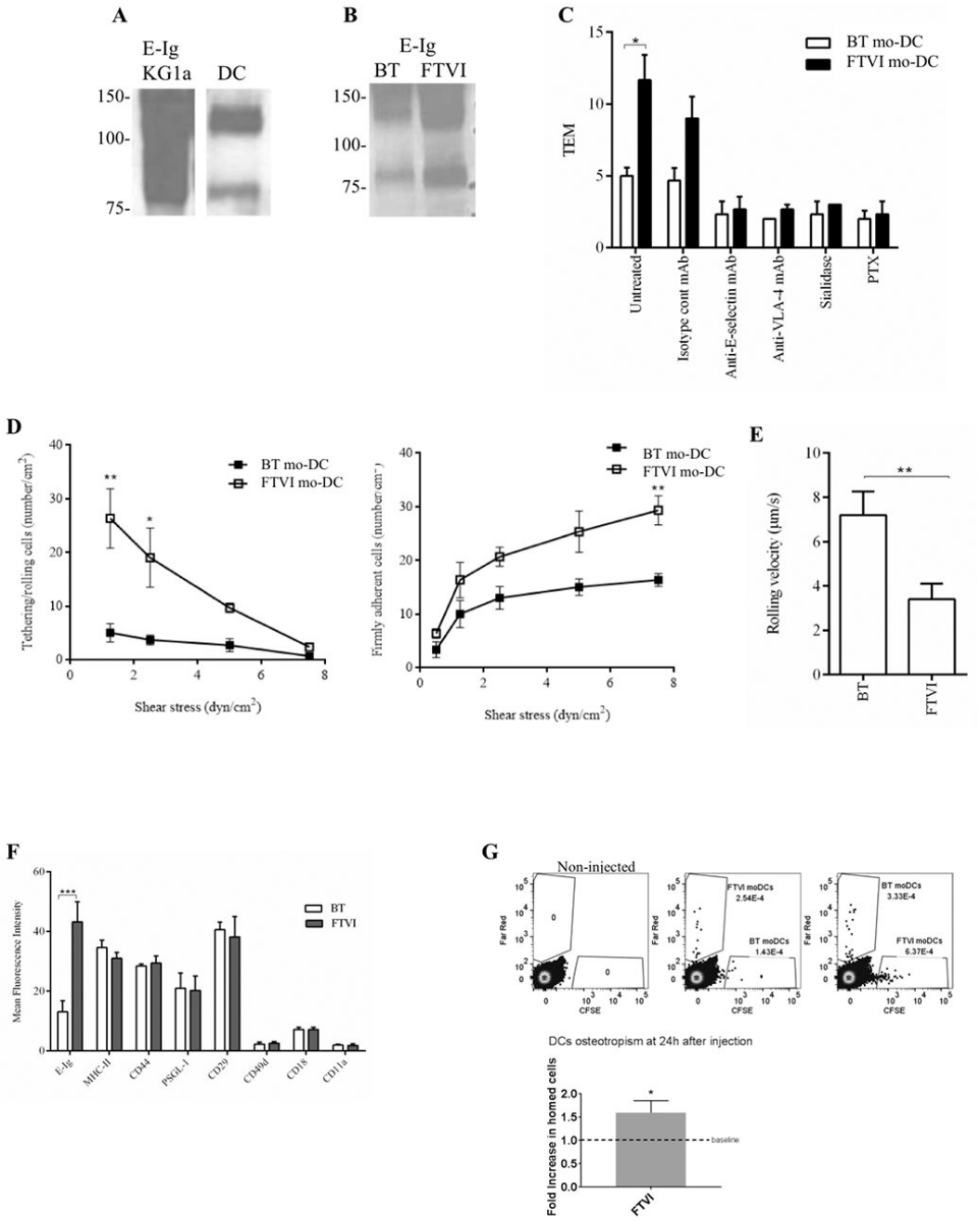


**Figure 6. Enforced fucosylation of human CD14-S mo-DCs yields higher E-selectin binding**

**(A)** *Western blot analysis comparing E-selectin binding (E-Ig reactivity) of KG1a and CD14-S mo-DCs*. Input lysates on each blot were normalized to equivalent cell numbers. **(B)** *Effects of exofucosylation on E-selectin ligand expression of mo-DCs*. CD14-S mo-DCs were buffer treated (BT) or FTVI-treated, and lysates (of equivalent cell numbers) were analyzed by Western blot for reactivity with E-Ig. **(C)** *Transendothelial migration (TEM) assay of buffer treated (BT) and FTVI-treated CD14-S mo-DCs*. The relative TEM value is the ratio of mo-DCs transmigrated on TNFα-stimulated HUVECs compared with mo-DCs transmigrated on non-stimulated HUVECs. TEM was assessed using mo-DCs (untreated),

HUVECs preincubated with function blocking anti-E-selectin mAb clone 68-5H11, mo-DCs preincubated with function blocking anti-VLA-4 mAb HP2/1 or isotype mAb, and mo-DCs treated with sialidase or PTX. **(D)** *Analysis of mo-DCs tethering/rolling interactions and firm adherence on TNFα-stimulated HUVEC monolayers under flow conditions. Left:* Shear stress was increased stepwise every 30 seconds, and the number of tethering/rolling cells per $cm^2$ of HUVEC was counted, during each 30 second segment. *Right*: At the end of each time segment, the number of cells that became firmly adhering per $cm^2$ area was measured. **(E)** *Average rolling velocity of BT- and FTVI-treated mo-DCs perfused over TNFα-stimulated HUVECs*. The velocity was estimated at 2.0 dyn/$cm^2$ flow, as the displacement of the centroid of the cell over 1 sec. Values are means ± SD (n= 3). Statistically significant differences are indicated by asterisks. **(F)** FTVI treatment does not affect cell surface protein expression. Flow cytometry analysis of E-Ig reactivity, MHC-II, CD44, PSGL-1, CD29, CD49d, CD18 and CD11a staining on buffer treated (BT, white bars) and FTVI-treated CD14-S mo-DCs (dark grey bars). Statistically significant differences are indicated by asterisks. **(G)** FTVI treatment of CD14-S mo-DCs improves their homing to bone marrow. FTVI-treated or buffer-treated (Unt) mo-DCs were labeled reciprocally with either CFSE or Far Red and mixed at 1:1 ratio. CFSE and Far Red labeled cells were retro-orbitally co-injected into NSG mice, with dye combination swapped between the mice. 24h after injection, bone marrow was harvested and the presence of labeled cells in BM was assessed by flow cytometry. At left, representative flow cytometry plots show mo-DCs migration to BM. At right, FTVI-treated mo-DCs show significantly increased BM homing compared to buffer treated-mo-DCs (baseline). Data are shown as mean ± SEM. *P*-values calculated by unpaired 2-tailed student's t-test (*, $P < 0.05$). Data are representative of 6 mice (3 mice for each dye combination).